Frequency versus Wave Vector for a
Diatomic Ionic Orthorhombic Biaxial Crystal

C. K. Asawa

Hughes Research Laboratories, Malibu, California 90265

(Received 12 May 1970)

Theoretical expressions are presented for the frequency ω versus the wave vector $\vec{k}$ resulting from the interaction between the electromagnetic field and an undamped vibrating diatomic ionic crystal with orthorhombic symmetry. The rigorous treatment using retarded electromagnetic fields shows that the resultant vibrations consist of a mixture of electromagnetic waves and mechanical lattice vibrations, as shown previously for cubic lattices in Huang's classic paper. Our treatment is applicable to biaxial crystals with orthorhombic symmetry. A systematic method for evaluating all cases is illustrated. It is noted that a theory for biaxial crystals with monoclinic and triclinic symmetries is complicated by the fact that the principal axes of physical properties are not simply oriented to the crystal axes.

INTRODUCTION

Prior to 1951, lattice vibrations invariably were calculated assuming only electrostatic interactions between ions. One principal result was the derivation of a relationship between the frequencies of the longitudinal and transverse optical waves, called the Lyddane-Sachs-Teller relationship.[1] Further theoretical advances resulted from the appearance of Huang's classic treatment[2] of the interaction between the lattice vibrations of a diatomic ionic crystal and a retarded electromagnetic field described by the complete set of Maxwell's equations. His detailed interpretation of the results emphasized two points: (a) The resultant vibrations consist of a mixture of electromagnetic waves and mechanical lattice vibrations, and (b) the optical waves just below the infrared dispersion frequency consist mainly of the mechanical transverse lattice vibrations. His calculations were limited to cubic crystals.

When anisotropic crystals are considered, it is found that the frequency of a vibration depends upon the orientation of the wave vector. Poulet's brief calculations[3] suggested this behavior. More extensive calculations were carried out by Merten[4] and by Loudon[5] for uniaxial crystals, using the Huang model. Merten limited his treatment to the electrostatic field case, while Loudon used the entire set of Maxwell's equations. Loudon also obtained approximate ω-versus-$\vec{k}$ expressions for right-angle Raman scattering for special limiting cases. The biaxial crystal was not examined.

Barker[6] has examined lattice vibration as in Huang's theory, but considers vibrational damping as well. This leads to the consideration of linewidths and to a modification of the ω-versus-k curves. For simplicity, however, only the undamped case will be considered here.

BRIEF RÉSUMÉ OF HUANG'S THEORY

Huang's treatment for cubic crystals is reviewed briefly here. The equation of motion for the lattice vibrations is given by

$$\ddot{\vec{W}} = b^{(1)}\vec{W} + b^{(2)}\vec{E} \ , \tag{1}$$

$$\vec{P} = b^{(3)}\vec{W} + b^{(4)}\vec{E} \ , \tag{2}$$

where $\vec{W} \equiv$ displacement between the negative and positive ions from the equilibrium positions multiplied by the square root of the ratio of the reduced mass of the two types of ions to the volume per ion pair, $\vec{E} \equiv$ macroscopic electric field (as used in Maxwell's equation), $\vec{P} \equiv$ dielectric polarization due to the generalized displacement $\vec{W}$ and the electronic polarization of the diatomic complex due to the electric field $\vec{E}$, and $b^{(m)} \equiv$ constant scalar factors, with $b^{(2)} = b^{(3)}$.

Assuming plane-wave solutions for $\vec{W}$, $\vec{E}$, and $\vec{P}$, with spatial and time dependence given by $\exp i(\vec{k} \cdot \vec{r} - \omega t)$, an expression is derived for the dielectric constant ϵ in terms of the $b^{(m)}$'s:

$$\epsilon = 1 + 4\pi P/E$$

or

$$\epsilon = 1 + 4\pi b^{(4)} + \frac{4\pi b^{(2)} b^{(3)}}{-b^{(1)} - \omega^2} \ . \tag{3}$$

This result is compared with the dispersion formula

$$\epsilon = \epsilon^{\infty} + \frac{\epsilon^0 - \epsilon^{\infty}}{1 - (\omega/\omega_0)^2} \ , \tag{4}$$

where ω_0 is the infrared dispersion frequency.

Comparison of (3) and (4) indicates that

$$b^{(1)} = -\omega_0^2 \ ,$$

$$b^{(2)} = b^{(3)} = [(\epsilon^0 - \epsilon^\infty)/4\pi]^{1/2} \omega_0 \ ,$$

$$b^{(4)} = (\epsilon^\infty - 1)/4\pi \ ,$$

where $\epsilon^0 \equiv$ static dielectric constant and $\epsilon^\infty \equiv$ high-frequency dielectric constant, where frequency is high relative to ω_0.

When the effect of retarded fields is considered, the complete set of Maxwell's equations is used in conjunction with (1) and (2). For plane-wave solutions Maxwell's equation results in

$$\vec{E} = -4\pi \frac{\vec{k}(\vec{k} \cdot \vec{P}) - (\omega^2/c^2)\vec{P}}{k^2 - \omega^2/c^2} \ , \tag{5}$$

where $\vec{k}$ is the wave vector.

Solution of (1), (2), and (5) results in

$$\omega^2 = (\epsilon^0/\epsilon^\infty)\,\omega_0^2 \equiv \omega^{l2} \tag{6}$$

for the longitudinal optical wave (LO) and

$$k^2c^2/\omega^2 = (\epsilon^0\omega_0^2 - \epsilon^\infty\omega^2)/(\omega_0^2 - \omega^2) \tag{7}$$

for the transverse optical wave (TO). The ω given by (6) is defined as the LO wave frequency ω^l. Equation (6) is the Lyddane-Sachs-Teller relationship; Eq. (7) is a quadratic equation in ω^2 yielding two values of ω^2.

The curves for (6) and (7) are shown in Fig. 1. The LO wave frequency given by (6) is nondegenerate. Each branch of the TO wave is doubly degenerate in frequency, although the degeneracy is not given by (7). The TO branches curve where the vibrations consist of a mixture of electromagnetic waves and mechanical lattice vibrations.

THEORY FOR BIAXIAL CRYSTALS WITH ORTHORHOMBIC SYMMETRY

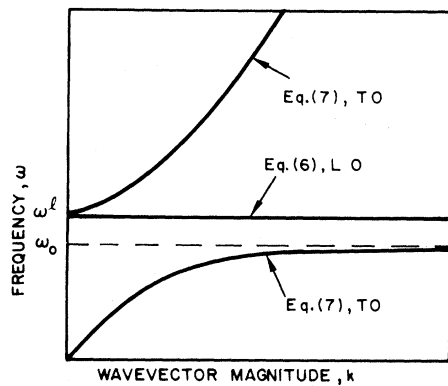The lattice vibrations and polarization equations for anisotropic crystals can be written in any rec-

FIG. 1. ω versus k given by (6) and (7) for a cubic system, for small values of k.

tangular coordinates as

$$\ddot{W}_i = \sum_{j=1}^{3} b_{ij}^{(1)} W_j + b_{ij}^{(2)} E_j \ , \tag{8}$$

$$P_i = \sum_{j=1}^{3} b_{ij}^{(3)} W_j + b_{ij}^{(4)} E_j \ , \tag{9}$$

where $i = 1, 2, 3$. These equations correspond to (1) and (2) for the cubic crystal. W_i, E_i, and P_i are now components of the ion-displacement (from equilibrium) vector, the electric field vector, and the polarization vector, respectively, in the rectangular coordinates. The $b_{ij}^{(m)}$'s are the second-rank tensors representing the physical properties connecting the components of the vectors $\vec{W}$, $\vec{E}$, and $\vec{P}$.

If all of the physical properties have the same unique set of principal axes, Eqs. (8) and (9) can be written along the principal axes in the diagonal form (i.e., only diagonal components of the transformed $b_{ij}^{(m)}$'s are nonzero). The W_i, E_i, and P_i components will also be described in the principal-axes coordinates. Neglecting new symbols for the new principal-axes coordinates, the transformed equations are written in diagonal form:

$$\ddot{W}_i = b_i^{(1)} W_i + b_i^{(2)} E_i \ , \tag{8'}$$

$$P_i = b_i^{(3)} W_i + b_i^{(4)} E_i \ , \tag{9'}$$

where $i = 1, 2, 3$. The $b_{ii}^{(m)}$ coefficient is written simply as $b_i^{(m)}$.

Plane-wave solutions for (8') and (9') are now assumed, with spatial and time dependence given by $\exp i(\vec{k} \cdot \vec{r} - \omega t)$. $\ddot{W}_i$ is then replaced by $-\omega^2 W_i$. Solving for P_i in terms of E_i, we have

$$P_i = [b_i^{(4)} + b_i^{(2)} b_i^{(3)}/(-b_i^{(1)} - \omega^2)] E_i \ . \tag{10}$$

The dielectric constant along the ith coordinate is then given by

$$\epsilon_i = 1 + 4\pi b_i^{(4)} + 4\pi b_i^{(2)} b_i^{(3)}/(-b_i^{(1)} - \omega^2) \ . \tag{11}$$

This result is compared with the dispersion formula for the ith coordinate:

$$\epsilon_i = \epsilon_i^\infty + \frac{\epsilon_i^0 - \epsilon_i^\infty}{1 - (\omega/\omega_i)^2} \ . \tag{12}$$

Then

$$b_i^{(1)} = -\omega_i^2 \ ,$$

$$b_i^{(4)} = b_i^{(3)} = [(\epsilon_i^0 - \epsilon_i^\infty)/4\pi]^{1/2} \omega_i \ , \tag{13}$$

$$b_i^{(4)} = (\epsilon_i^\infty - 1)/4\pi \ ,$$

where $\omega_i \equiv$ the characteristic lattice vibrational frequency in the ith direction in the absence of the long-range electric field component, $\epsilon_i^0 \equiv$ static dielectric constant in the ith direction, and ϵ_i^∞ $\equiv$ high-frequency dielectric constant in the ith di-

rection.

It can be shown by energy-density consideration that $b_i^{(2)}$ is equal to $b_i^{(3)}$, as has been described by Huang for the cubic crystal and by Merten for the anisotropic crystal (using a dyadic formulation).

The validity of describing the lattice vibration and polarization equation in the diagonal forms (8') and (9') depends on the assumption that all the physical properties $b^{(m)}$'s have the same principal axes. Equations (13) show that the $b^{(m)}$'s are functions of the dielectric constants at two different frequencies and of the characteristic vibrational frequencies. This suggests that the dielectric constants at the two different frequencies and the characteristic frequencies also must be diagonal along the same principal axis in order for the assumption to hold that the $b_{ij}^{(m)}$'s can be diagonalized simultaneously. This can occur in biaxial crystals with orthorhombic symmetry,[7] but not in biaxial crystals with monoclinic or triclinic symmetry.

A third set of three equations is given by Maxwell's equation. Assuming plane-wave solutions, the component equations corresponding to (5) are given by

$$E_i = -4\pi \frac{k_i(\vec{k} \cdot \vec{P}) - (\omega^2/c^2)P_i}{k^2 - \omega^2/c^2} \qquad (14)$$

for $i = 1, 2, 3$. k_i is the ith component of the wave vector $\vec{k}$. E_i from (10) is substituted for E_i in (14). The following expression for P_i in terms of k_i results:

$$\left((\omega_i^2 - \omega^2) - \frac{\omega^2}{c^2 k^2} (\epsilon_i^0 \omega_i^2 - \epsilon_i^\infty \omega^2) \right) P_i = [(\omega_i^2 - \omega^2)$$

$$- (\epsilon_i^0 \omega_i^2 - \epsilon_i^\infty \omega^2)] \frac{k_i}{k^2} (\vec{k} \cdot \vec{P}), \qquad i = 1, 2, 3 \quad . \quad (15)$$

These are the three basic equations.

If each of the coefficients of P_i is nonzero, P_i can be written as

$$P_i = \frac{(\omega_i^2 - \omega^2) - (\epsilon_i^0 \omega_i^2 - \epsilon_i^\infty \omega^2)}{(\omega_i^2 - \omega^2) - (\omega^2/c^2 k^2)(\epsilon_i^0 \omega_i^2 - \epsilon_i^\infty \omega^2)} \frac{k_i}{k^2} (\vec{k} \cdot \vec{P}),$$

$$i = 1, 2, 3 \quad . \quad (16)$$

Multiplying both sides by k_i and summing on i results in

$$\sum_{i=1}^{3} k_i P_i = \sum_{i=1}^{3} \frac{(\omega_i^2 - \omega^2) - (\epsilon_i^0 \omega_i^2 - \epsilon_i^\infty \omega^2)}{(\omega_i^2 - \omega^2) - (\omega^2/c^2 k^2)(\epsilon_i^0 \omega_i^2 - \epsilon_i^\infty \omega^2)}$$

$$\times \frac{k_i^2}{k^2} (\vec{k} \cdot \vec{P}) \quad .$$

However, $\sum k_i P_i = (\vec{k} \cdot \vec{P})$. In general, $\vec{k} \cdot \vec{P} \neq 0$; then

$$\sum_{i=1}^{3} \frac{(\omega_i^2 - \omega^2) - (\epsilon_i^0 \omega_i^2 - \epsilon_i^\infty \omega^2)}{(\omega_i^2 - \omega^2) - (\omega^2/c^2 k^2)(\epsilon_i^0 \omega_i^2 - \epsilon_i^\infty \omega^2)} \frac{k_i^2}{k^2} = 1 \quad . \quad (17)$$

Each of the denominators (i.e., for each value of i) must be nonzero. $k_i/k = \cos\phi_i$, the direction cosines of the wave vector $\vec{k}$. Note that $\sum k_i^2 = k^2$ was used above. Equations (15) and (17) are used extensively later, where examples for various orientations of the wave vector $\vec{k}$ are illustrated.

It is noted immediately that $\omega^2 = c^2 k^2$ satisfies (17). This is a root of (17). The remaining five roots for ω^2 are obtained by multiplying out (17). This results in

$$\left(\frac{\omega^2}{c^2 k^2} - 1 \right) \text{(fifth-degree polynomial in } \omega^2) = 0 \quad .$$

The first factor gives the $\omega^2 = c^2 k^2$ root which, of course, is the frequency-velocity relation for wave propagation in vacuum. We thus disregard this solution. The second factor set to zero gives the desired five ω-versus-k branches.

SYMMETRY CONSIDERATIONS AND POLARIZATION DIRECTIONS

Some insight on the polarization directions of the lattice vibration is gained from the $k = 0$ group-theoretical analysis. There are three symmetry classes belonging to the orthorhombic system: (i) the $mm2$ or C_{2v} class; (ii) the 222 or D_2 class; (iii) the mmm or D_{2h} class. The vibrational motion of the two-ion molecules located in an orthorhombic environment yields the following results: (a) the $mm2$ or C_{2v} class: The reducible optical vibration Γ_{vib} is decomposable into three irreducible representations of C_{2v}, i.e., $\Gamma_{vib} = A_1(x_3) + B_1(x_1) + B_2(x_2)$. There are three infrared-active optical vibrational modes; one is polarized along the x_1 axis, another along the x_2 axis, and the third along the x_3 axis. (b) The 222 or D_2 class: There are two infrared-active optical vibrational modes. If the ions in equilibrium lie along one of the crystalline axes, the polarization directions of the two infrared-active modes are along the other two crystalline axes. This is also described as follows: If the ions, for example, lie along the x_3 axis in equilibrium, then $\Gamma_{vib} = A + B_2(x_2) + B_3(x_1)$. The A mode is not infrared active (but is Raman active). (c) The mmm or D_{2h} class: There are no infrared-active modes for our crystal model. The three optical vibrations are Raman active, however. In this case $\Gamma_{vib} = B_{3g} + B_{2g} + A_g$.

The components P_i of the polarization vector $\vec{P}$ along the orthorhombic crystalline coordinates will constitute the basis for the description of the examples given below. This choice occurs natur-

ally because the polarization directions of the in-
frared vibrational modes are directed along the
crystalline axes in this approximation. In addi-
tion, the characteristic vibrational frequencies and
dielectric constants are also directly identified
with the crystalline axial direction.

The above description for the orthorhombic case
is compared with that for the cubic crystal where
all directions are equivalent; three mutually per-
pendicular polarization components are chosen
such that two components are perpendicular to the
wave vector $\vec{k}$ and the third component parallel to
$\vec{k}$. The first two components lead to doubly de-
generate TO waves, and the third component leads
to the LO wave. The choice of polarization com-
ponents is also compared with the uniaxial case
where two mutually perpendicular polarization
components are taken to lie in the $x_1 x_2$ plane, the
plane being perpendicular to the x_3 or crystalline
c axis. One of these components is oriented to be
perpendicular to the general wave vector $\vec{k}$; this
gives the TO wave. The third component is taken
to be along the x_3 or c axis.

EXAMPLES OF USE OF EQS. (15) AND (17) FOR ORTHO-RHOMBIC BIAXIAL, UNIAXIAL, AND CUBIC CRYSTALS FOR VARIOUS ORIENTATIONS OF WAVE VECTOR $\vec{k}$

ω-versus-k expressions are obtained for three
different orientations of the wave vector $\vec{k}$ for the
orthorhombic crystal. The three orientations
are sufficient to illustrate all possible cases.
The uniaxial and cubic cases are obtained by con-
sidering special polarization component directions
as described above; these cases are also described
here.

Case I. Orthorhombic Biaxial Crystal (General $\vec{k}$ and $\vec{P}$ with Nonzero Components)

$\vec{k} = (k_1, k_2, k_3)$, $\vec{P} = (P_1, P_2, P_3)$. The components
are given in the x_1, x_2, x_3 coordinate system. This
is shown in Fig. 2. [In the following discussion
when a vector component is meant, the component
will be written as a vector (i.e., $\vec{k}_i$ or $\vec{P}_i$). Oth-
erwise k_i or P_i are scalar quantities.]

The general solution of (17) is used because
none of the k_i components is zero. The direction
cosines of $\vec{k}$ are given by $\cos\phi_i = (k_i/k)$; then (17)
is written as

$$\frac{(\omega_1^2 - \omega^2) - (\epsilon_1^0 \omega_1^2 - \epsilon_1^\infty \omega^2)}{(\omega_1^2 - \omega^2) - (\omega^2/c^2 k^2)(\epsilon_1^0 \omega_1^2 - \epsilon_1^\infty \omega^2)} \cos^2\phi_1$$

$$+ \frac{(\omega_2^2 - \omega^2) - (\epsilon_2^0 \omega_2^2 - \epsilon_2^\infty \omega^2)}{(\omega_2^2 - \omega^2) - (\omega^2/c^2 k^2)(\epsilon_2^0 \omega_2^2 - \epsilon_2^\infty \omega^2)} \cos^2\phi_2$$

$$+ \frac{(\omega_3^2 - \omega^2) - (\epsilon_3^0 \omega_3^2 - \epsilon_3^\infty \omega^2)}{(\omega_3^2 - \omega^2) - (\omega^2/c^2 k^2)(\epsilon_3^0 \omega_3^2 - \epsilon_3^\infty \omega^2)} \cos^2\phi_3 = 1 \ . \quad (18)$$
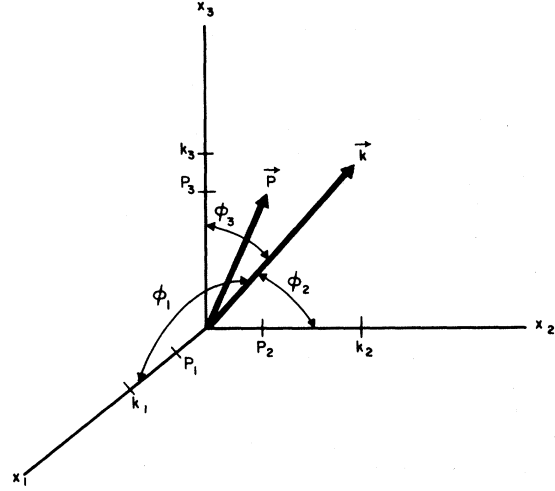

FIG. 2. Geometry of the orthorhombic case I for a
general orientation of $\vec{k}$, i.e., each k_i component is
nonzero.

Because $\cos^2\phi_1 + \cos^2\phi_2 + \cos^2\phi_3 = 1$, only two an-
gles are necessary to orient $\vec{k}$. For a given value
of $\vec{k}$ where no k_i component is zero, (18) is a
sixth-degree equation in ω^2, yielding six solutions
for ω^2. One of the roots is $\omega^2 = c^2 k^2$, as discussed
above. This root is discarded.

A transverse lattice wave is defined as that in
which the wave vector $\vec{k}$ is perpendicular to a
component $\vec{P}_i$ of the polarization vector $\vec{P}$. There
is no $\vec{P}_i$ component in the x_1, x_2, x_3 coordinate
system perpendicular to $\vec{k}$ (because $k_i \neq 0$ for any
i's); hence no TO wave is observed. It is noted
that the "purely electromagnetic" wave for large
ω and k has the wave vector $\vec{k}$ perpendicular to
$\vec{D}$, the electric displacement vector, but not per-
pendicular to a component of $\vec{P}$ for this case.

The fifth-degree equation obtained from (18)
yields five ω-versus-$\vec{k}$ branches. As an example
we have indicated a particular set of solutions in
Fig. 3. The long-range electric forces have been
assumed to be greater than the short-range aniso-
tropy forces, so that the ω_i's are grouped together
as are the ω_i^l's at $k = 0$. In addition, it has been
arbitrarily assumed that $\epsilon_1^0/\epsilon_1^\infty \gg \epsilon_2^0/\epsilon_2^\infty \gg \epsilon_3^0/\epsilon_3^\infty$, so
that the ω_i^l's are arranged as indicated in Fig. 3.

It is noted that all five branches interact strong-
ly for small k values. All of the branches con-
sist of mixed electromagnetic and mechanical vi-
brations for these k values. These waves are
neither longitudinal nor transverse in the $\vec{k} \perp \vec{P}_i$
sense.

Case II. Orthorhombic Biaxial Crystal ($\vec{k}$ in a Plane Formed by Two of the Principal Axes)
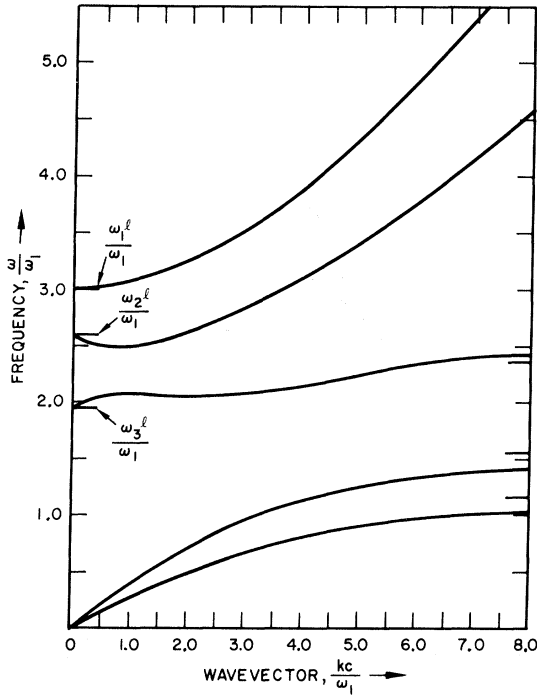
One of the k_i components is zero (e.g., $k_i = 0$);

FIG. 3. ω versus k for small-k values for general $\vec{k}$ orientation. Orthorhombic case I. Parameter values used: $\epsilon_1^\infty = 2$, $\epsilon_2^\infty = 3$, $\epsilon_3^\infty = 4$, $\epsilon_1^0 = 18$, $\epsilon_2^0 = 12$, $\epsilon_3^0 = 6$, $\omega_2 = 1.3\omega_1$, $\omega_3 = 1.6\omega_1$. $\phi_1 = \phi_2 = \phi_3$.

then $\vec{k}$ is in the $x_2 x_3$ plane. $\vec{k} = (0, k_2, k_3)$, and $\vec{P} = (P_1, P_2, P_3)$. This case is shown in Fig. 4.

Because $k_1 = 0$, the coefficient of P_1 in (15) must be zero:

$$(\omega_1^2 - \omega^2) - (\omega^2/c^2 k^2)(\epsilon_1^0 \omega_1^2 - \epsilon_1^\infty \omega^2) = 0 \quad . \quad (19)$$

This gives the frequencies of the transverse waves. The component P_1 of the dielectric polarization vector is along x_1 and is perpendicular to $\vec{k}$. Equation (19) yields two of the transverse solutions. The "purely electromagnetic" waves for large ω and k are also "transverse" in the $\vec{k} \perp \vec{P}_1$ component sense; in this case, $\vec{P}_1 \parallel \vec{E}_1 \parallel \vec{D}_1$.

The $k_1 = 0$ component resulted in (19), which gave two values for frequency versus k. The other three frequencies are given by (17) (noting that the $i = 1$ term vanishes because $k_1 = 0$):

$$\frac{(\omega_2^2 - \omega^2) - (\epsilon_2^0 \omega_2^2 - \epsilon_2^\infty \omega^2)}{(\omega_2^2 - \omega^2) - (\omega^2/c^2 k^2)(\epsilon_2^0 \omega_2^2 - \epsilon_2^\infty \omega^2)} \cos^2\phi_2$$

$$+ \frac{(\omega_3^2 - \omega^2) - (\epsilon_3^0 \omega_3^2 - \epsilon_3^\infty \omega^2)}{(\omega_3^2 - \omega^2) - (\omega^2/c^2 k^2)(\epsilon_3^0 \omega_3^2 - \epsilon_3^\infty \omega^2)} \cos^2\phi_3 = 1 \quad . \quad (20)$$

Because $\cos\phi_1 = 0$, $\cos^2\phi_2 = \sin^2\phi_3$. Equation (20) is a quartic equation in ω^2 and gives the other three branches of the ω-versus-k curves. The fourth solution is the $\omega^2 = c^2 k^2$ root, discussed

above. It is noted that the waves are *neither* longitudinal nor transverse (in the $\vec{k} \parallel \vec{P}_i$ or the $\vec{k} \perp \vec{P}_i$ sense). For large-k values two of the roots give the frequencies of the mechanical lattice vibrations; the other root gives the frequency of the purely electromagnetic wave. The results are shown graphically in Fig. 5. The three branches obtained from (20) interfere or interact with each other in the region of small-k values where the waves are mixtures of electromagnetic and mechanical vibrations. The interaction manifests itself in the "repulsion" or "attraction" of the branches.

It is noted that the two transverse waves obtained from (19) do not interfere with the three waves obtained from (20); the two equations are independent of each other. This is shown more clearly in Fig. 6; here the dielectric constants were assumed to be different from those for the TO wave of Fig. 5 so that the upper branch is lowered. Level crossings of the TO branches given by (19) with the three branches given by (20) are shown.

Case III. Orthorhombic Biaxial Crystal ($\vec{k}$ along One of the Principal Axes)

When two of the k_i components are zero, we have, for example, $\vec{k} = (0, 0, k_3)$, $\vec{P} = (P_1, P_2, P_3)$. The orientation of the vectors of case III is shown in Fig. 7.

$k_1 = 0$ and $k_2 = 0$; the coefficients of P_1 and P_2 are then set equal to zero in (15):

$$(\omega_1^2 - \omega^2) - (\omega^2/c^2 k^2)(\epsilon_1^0 \omega_1^2 - \epsilon_1^\infty \omega^2) = 0 \quad (21)$$

and

$$(\omega_2^2 - \omega^2) - (\omega^2/c^2 k^2)(\epsilon_2^0 \omega_2^2 - \epsilon_2^\infty \omega^2) = 0 \quad . \quad (22)$$
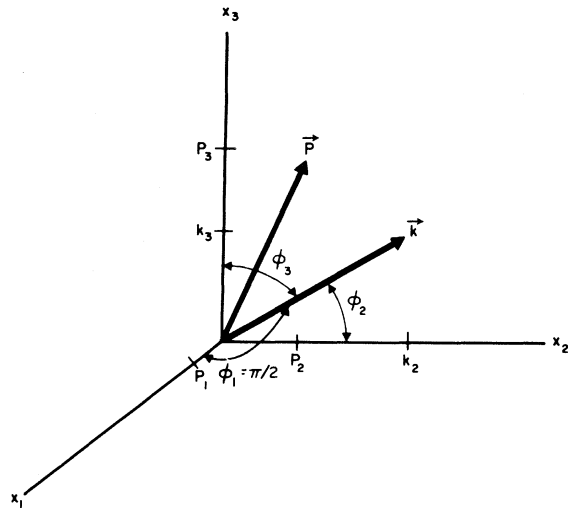

FIG. 4. Geometry of the orthorhombic case II where $\vec{k}$ lies in the $x_2 x_3$ plane.

Equation (21) gives the transverse solutions for $\vec{k} \perp \vec{P}_1$, and (22) gives the transverse solutions for $\vec{k} \perp \vec{P}_2$. Each equation again yields two solutions. The fifth root is given by (17) because $k_3 \neq 0$:

$$\frac{(\omega_3^2 - \omega^2) - (\epsilon_3^0 \omega_3^2 - \epsilon_3^\infty \omega^2)}{(\omega_3^2 - \omega^2) - (\omega^2/c^2 k^2)(\epsilon_3^0 \omega_3^2 - \epsilon_3^\infty \omega^2)} = 1 \quad ,$$

(23)

$$\omega^2 = \omega_3^2 (\epsilon_3^0/\epsilon_3^\infty) \equiv \omega_3^{l2} \quad .$$

The longitudinal frequency is defined by the symbol ω_3^l. For this case $\vec{k}$ is parallel to $\vec{P}_3$. Equation (23) is the well-known Lyddane-Sachs-Teller relationship between the LO and TO frequencies, cited previously. The three sets of branches are noninteracting and the branches may cross when sets of parameters other than those for Fig. 8 are used.

Cases I–III describe all possible cases for the biaxial orthorhombic crystal. The ω-versus-k values for case I require the solution of a fifth-degree equation. All solutions are real, so that the computations are relatively simple. We now describe the use of (15) and (17) for the uniaxial and cubic crystals as special cases.
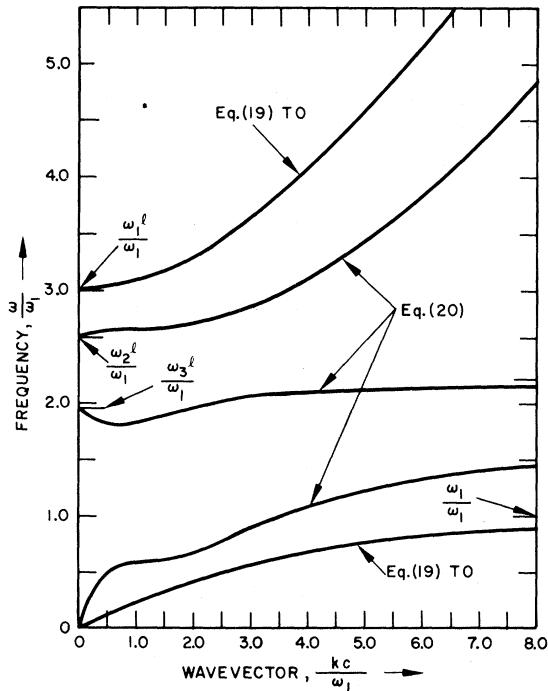

FIG. 5. ω versus k for small-k values for $\vec{k}$ in the $x_2 x_3$ plane. Orthorhombic case II. Parameter values same as for Fig. 3. $\epsilon_1^\infty = 2$, $\epsilon_2^\infty = 3$, $\epsilon_3^\infty = 4$, $\epsilon_1^0 = 18$, $\epsilon_2^0 = 12$, $\epsilon_3^0 = 6$, $\omega_2 = 1.3\omega_1$, $\omega_3 = 1.6\omega_1$. The branches do not cross because of the particular parameter values chosen. $\phi_2 = \phi_3$.
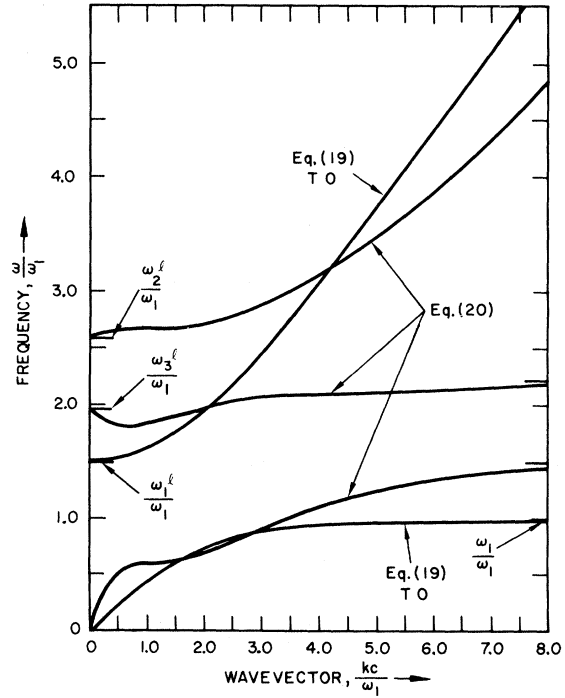

FIG. 6. Same as Fig. 5 except that ϵ_1^∞ and ϵ_1^0 were changed in order to illustrate that the two transverse branches do cross the other three branches $\epsilon_1^\infty = 2$, $\epsilon_1^0 = 4.5$. The crossing occurs because (19) is independent of (20).

Case IV. Uniaxial Crystal Application of Eqs. (15) and (17)

For the uniaxial case any direction in the $x_1 x_2$ plane is equivalent for macroscopic physical properties or the electromagnetic field vectors. For a given arbitrary k vector, we can then select an axis $0x_a$ in the $x_1 x_2$ plane such that $\vec{0 x_a} \perp \vec{k}$. Then let $0x_b$ be an axis in the $x_1 x_2$ plane perpendicular to $0x_a$. In the x_a, x_b, x_3 coordinates the $\vec{k}$ and $\vec{P}$ vectors are written as

$$\vec{k} = (0, k_b, k_3), \quad \vec{P} = (P_a, P_b, P_3) \quad .$$

This case is shown in Fig. 9.

In (15) and (17) the indices now run from $i = a$, b, 3. Because any direction in the $x_1 x_2$ plane or the $x_a x_b$ plane is equivalent,

$$\omega_1 = \omega_2 = \omega_a = \omega_b, \quad \epsilon_1^0 = \epsilon_2^0 = \epsilon_a^0 = \epsilon_b^0, \quad \epsilon_1^\infty = \epsilon_2^\infty = \epsilon_a^\infty = \epsilon_b^\infty \quad .$$

Because $k_a = 0$, the coefficient of P_a in (15) is set to zero ($i = 1$ is replaced by $i = a$):

$$(\omega_a^2 - \omega^2) - (\omega^2/c^2 k^2)(\epsilon_a^0 \omega_a^2 - \epsilon_a^\infty \omega^2) = 0 \quad . \quad (24)$$

This corresponds to the transverse wave where $\vec{k} \perp \vec{P}_a$. There are two solutions to (24). The other three frequencies are given by (17) (where $i = 2$ is
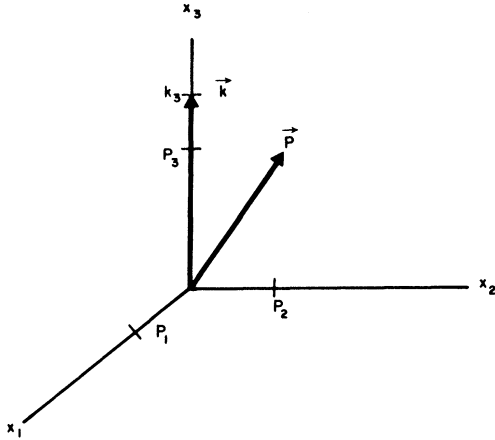
FIG. 7. Geometry of the orthorhombic case III where $\vec{k}$ is along the x_3 axis.

replaced by $i = b$). Then

$$\frac{(\omega_a^2 - \omega^2) - (\epsilon_a^0 \omega_a - \epsilon_a^\infty \omega^2)}{(\omega_a^2 - \omega^2) - (\omega^2/c^2 k^2)(\epsilon_a^0 \omega_a^2 - \epsilon_a^\infty \omega^2)} \sin^2\phi_3$$

$$+ \frac{(\omega_3^2 - \omega^2) - (\epsilon_3^0 \omega_3^2 - \epsilon_3^\infty \omega^2)}{(\omega_3^2 - \omega^2) - (\omega^2/c^2 k^2)(\epsilon_3^0 \omega_3^2 - \epsilon_3^\infty \omega^2)} \cos^2\phi_3 = 1 \ , \quad (25)$$

because $\cos^2\phi_b = \sin^2\phi_3$ and $\omega_b = \omega_a$, $\epsilon_b^0 = \epsilon_a^0$, $\epsilon_b^\infty = \epsilon_a^\infty$. This is a quartic equation in ω^2, yielding
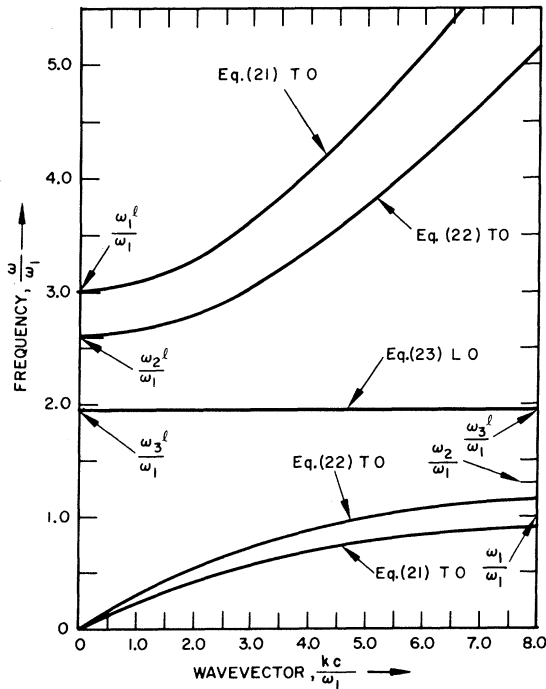

FIG. 8. ω versus k for small-k values for $\vec{k}$ along the x_3 axis. Orthorhombic case III. Same parameters as for Figs. 3 and 5. The three sets of branches may cross with other choices of parameters.

four roots. Three of the solutions give three ω-versus-k branches. The other solution is the $\omega = ck$ root. Because $\vec{k}$ is inclined at an arbitrary angle with respect to $\vec{P}_b$ and $\vec{P}_3$, the waves are neither longitudinal nor transverse. Typical ω-versus-$\vec{k}$ curves for the uniaxial case are given by Loudon.[5]

Case V. Uniaxial Crystal ($\vec{k}$ Perpendicular to the x_3 or c Axis)

When $\vec{k}$ lies in the $x_1 x_2$ or $x_a x_b$ plane, denote $\vec{k}$ by $\vec{k} = (0, k_b, 0)$. Write $\vec{P}$ as $\vec{P} = (P_a, P_b, P_3)$ (shown in Fig. 10). Then in (15) the coefficients of P_a and P_3 are set equal to zero, yielding

$$(\omega_a^2 - \omega^2) - (\omega^2/c^2 k^2)(\epsilon_a^0 \omega_a^2 - \epsilon_a^\infty \omega^2) = 0 \qquad (26)$$

and

$$(\omega_3^2 - \omega^2) - (\omega^2/c^2 k^2)(\epsilon_3^0 \omega_3^2 - \epsilon_3^\infty \omega^2) = 0 \ . \qquad (27)$$

These are the two sets of transverse waves with two solutions each.

The other solution is the longitudinal solution obtained from (17) evaluated with $i = b$ the only nonvanishing term:

$$\frac{(\omega_b^2 - \omega^2) - (\epsilon_b^0 \omega_b^2 - \epsilon_b^\infty \omega^2)}{(\omega_b^2 - \omega^2) - (\omega^2/c^2 k^2)(\epsilon_b^0 \omega_b^2 - \epsilon_b^\infty \omega^2)} = 1$$

or

$$(\omega^2/c^2 k^2 - 1)(\epsilon_b^0 \omega_b^2 - \epsilon_b^\infty \omega^2) = 0 \ .$$

The second factor set equal to zero gives the longitudinal solution for this k-vector orientation:

$$\omega^2 = (\epsilon_b^0/\epsilon_b^\infty) \omega_b^2 \equiv \omega_b^{l2} \ . \qquad (28)$$

Case VI. Uniaxial Crystal ($\vec{k}$ along x_3 Axis in $x_a x_b x_3$ Coordinate System)

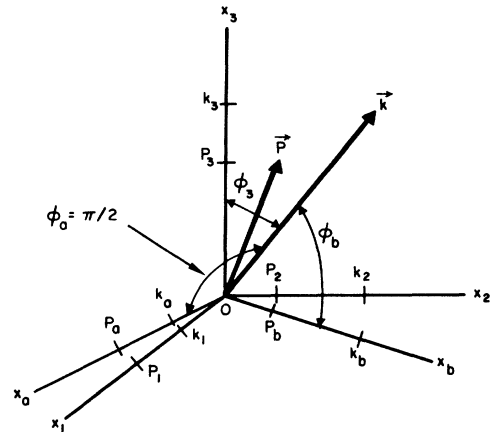$\vec{k} = (0, 0, k_3)$, $\vec{P} = (P_a, P_b, P_3)$. This is illustrated

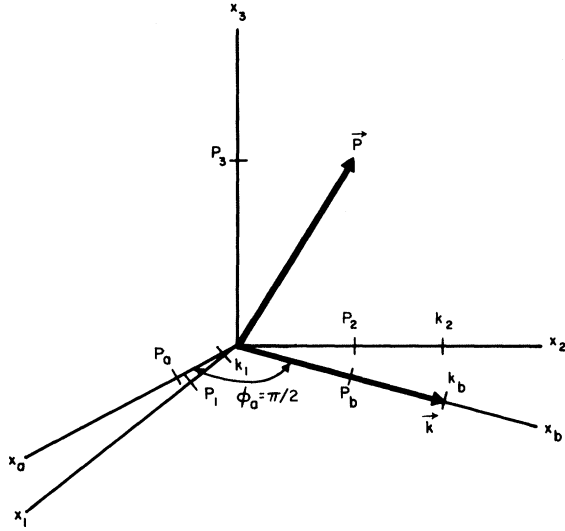FIG. 9. Special polarization component directions with respect to a general $\vec{k}$ vector. Uniaxial case IV.

FIG. 10. Special polarization component directions for $\vec{k}$ in the $x_1 x_2$ plane. Uniaxial case V.

in Fig. 11. Note that the x_a, x_b coordinates are equivalent to the x_1, x_2 coordinates (i.e., either pair yields the same set of equations). Because $k_a = k_b = 0$, the coefficients of P_a and P_b in (15) are set equal to zero:

$$(\omega_a^2 - \omega^2) - (\omega^2/c^2 k^2)(\epsilon_a^0 \omega_a^2 - \epsilon_a^\infty \omega^2) = 0 \qquad (29)$$

and

$$(\omega_b^2 - \omega^2) - (\omega^2/c^2 k^2)(\epsilon_b^0 \omega_b^2 - \epsilon_b^\infty \omega^2) = 0 \quad . \qquad (30)$$

These transverse waves are degenerate because $\omega_a = \omega_b$, $\epsilon_a^0 = \epsilon_b^0$, and $\epsilon_a^\infty = \epsilon_b^\infty$. A pair of doubly degenerate transverse-wave solutions are obtained from (29) and (30).

The other solution is obtained from (17) because $k_3 \neq 0$.

$$\frac{(\omega_3^2 - \omega^2) - (\epsilon_3^0 \omega_3^2 - \epsilon_3^\infty \omega^2)}{(\omega_3^2 - \omega^2) - (\omega^2/c^2 k^2)(\epsilon_3^0 \omega_3^2 - \epsilon_3^\infty \omega^2)} = 1$$

or

$$(\omega^2/c^2 k^2 - 1)(\epsilon_3^0 \omega_3^2 - \epsilon_3^\infty \omega^2) = 0 \quad .$$

The second factor set to zero gives the longitudinal frequency along the x_3 axis:

$$\omega^2 = (\epsilon_3^0/\epsilon_3^\infty) \omega_3^2 \equiv \omega_3^{l2} \quad . \qquad (31)$$

Case VII. Cubic

All directions are equivalent for macroscopic physical properties and the electromagnetic field vectors.

The polarization vectors can be written in terms of any two mutually perpendicular directions

which are perpendicular to $\vec{k}$, e.g., $0x_c$ and $0x_d$. Replace $i = 1$, 2, 3 by $i = c$, d, e in (15) and (17). We have $k = (0, 0, k_e)$, $\vec{P} = (P_c, P_d, P_e)$.

Since $k_c = k_d = 0$, the coefficients of P_c and P_d in (15) are zero. This results in the transverse waves

$$(\omega_c^2 - \omega^2) - (\omega^2/c^2 k^2)(\epsilon_c^0 \omega_c^2 - \epsilon_c^\infty \omega^2) = 0 \qquad (32)$$

and

$$(\omega_d^2 - \omega^2) - (\omega^2/c^2 k^2)(\epsilon_d^0 \omega_d^2 - \epsilon_d^\infty \omega^2) = 0 \quad . \qquad (33)$$

This describes the two cases where $\vec{k} \perp P_c$ and $\vec{k} \perp P_d$. In the cubic crystal $\omega_c = \omega_d = \omega_e$, $\epsilon_c^0 = \epsilon_d^0 = \epsilon_e^0$, $\epsilon_c^\infty = \epsilon_d^\infty = \epsilon_e^\infty$. Then (32) and (33) are degenerate, i.e., the ω-versus-k values for the transverse waves are doubly degenerate.

Because $k_c \neq 0$, Eq. (17) gives

$$\omega^2 = (\epsilon_c^0/\epsilon_c^\infty) \omega_c^2 \equiv \omega_c^{l2} \quad . \qquad (34)$$

This is the frequency of the longitudinal wave, as can be seen in Fig. 12, where $\vec{k} \parallel \vec{P}_e$. Equations (32) and (33) and Eq. (34) are precisely the same as (7) and (6), respectively, for the cubic-crystal case.

APPLICATION TO RIGHT-ANGLE RAMAN SCATTERING

Phonons causing right-angle Raman scattering have wave-vector magnitudes of approximately $|\vec{k}| = 3 \times 10^5$ cm^{-1} and frequency ω of the order of 2×10^{14} sec^{-1}. Thus we can write $ck \gg \omega$. These phonons are located near the right-hand edge of Figs. 1, 3, 5, 6, and 8 and consist dominantly of
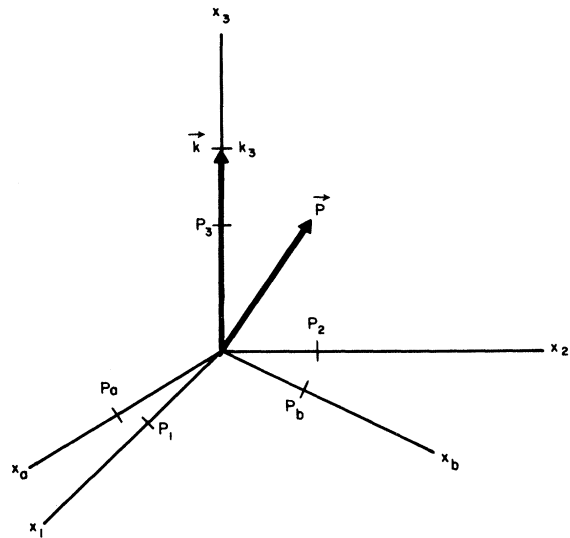

FIG. 11. Special polarization component directions for $\vec{k}$ along the x_3 direction. Uniaxial case VI.
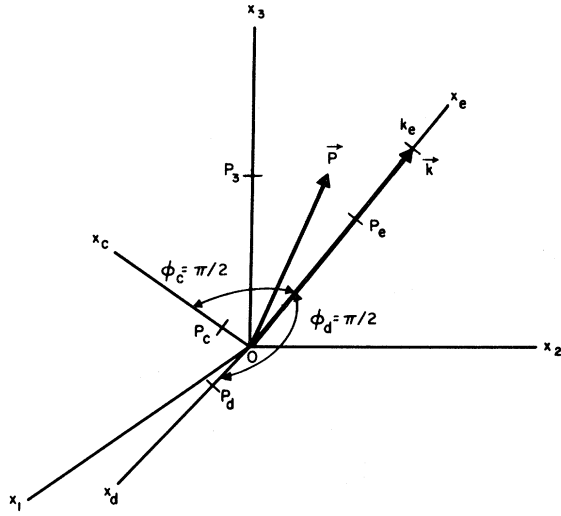
FIG. 12. Special polarization component direction with respect to the general $\vec{k}$ vector. Cubic case VII.

mechanical lattice vibrations and a very small mixture of electromagnetic radiation. The frequencies for these cases can be calculated by letting the terms containing the factors $(\omega^2/c^2 k^2)$

vanish in (15) and (17). Equation (15) becomes

$$(\omega_i^2 - \omega^2) P_i = [(\omega_i^2 - \omega^2) - (\epsilon_i^0 \omega_i^2 - \epsilon_i^\infty \omega^2)]$$

$$\times (k_i/k^2)(\vec{k} \cdot \vec{P}), \quad i = 1, 2, 3 \qquad (35)$$

and (17) becomes

$$\sum_{i=1,2,3} \frac{(\epsilon_i^0 \omega_i^2 - \epsilon_i^\infty \omega^2)}{(\omega_i^2 - \omega^2)} \frac{k_i^2}{k^2} = 0 \quad . \qquad (36)$$

These equations are evaluated in the same manner as in cases I–VII. Equation (36) is now only cubic in ω^2, simplifying the calculation somewhat. The direction cosines of the wave vector k are given by $\cos\phi_i = (k_i/k)$. As the orientation of $\vec{k}$ is changed in an orthorhombic crystal, the solutions of (35) and (36) manifest how the frequency of the observed Raman line changes.

Equation (36) is a third-degree equation in ω^2. If we let the solution be ω_a^2, ω_b^2, and ω_c^2, we obtain a modified Lyddane-Sachs-Teller relation for the orthorhombic case:

$$\frac{\omega_a^2 \omega_b^2 \omega_c^2}{\omega_1^2 \omega_2^2 \omega_3^2} = \frac{\epsilon_1^0 \cos^2\phi_1 + \epsilon_2^0 \cos^2\phi_2 + \epsilon_3^0 \cos^2\phi_3}{\epsilon_1^\infty \cos^2\phi_1 + \epsilon_2^\infty \cos^2\phi_2 + \epsilon_3^\infty \cos^2\phi_3} \quad . \qquad (37)$$

Other relationships are easily obtained. The sum of the solutions is given by

$$\omega_a^2 + \omega_b^2 + \omega_c^2 = \frac{[\epsilon_1^0 \omega_1^2 + \epsilon_1^\infty(\omega_2^2 + \omega_3^2)]\cos^2\phi_1 + [\epsilon_2^0 \omega_2^2 + \epsilon_2^\infty(\omega_1^2 + \omega_3^2)]\cos^2\phi_2 + [\epsilon_3^0 \omega_3^2 + \epsilon_3^\infty(\omega_1^2 + \omega_2^2)]\cos^2\phi_3}{\epsilon_1^\infty \cos^2\phi_1 + \epsilon_2^\infty \cos^2\phi_2 + \epsilon_3^\infty \cos^2\phi_3} \quad . \qquad (38)$$

A third relation for an orthorhombic crystal is finally obtained:

$$\omega_a \omega_b + \omega_a \omega_c + \omega_b \omega_c$$

$$= \frac{[\epsilon_1^\infty \omega_2^2 \omega_3^2 + \epsilon_1^0 \omega_1^2(\omega_2^2 + \omega_3^2)]\cos^2\phi_1 + [\epsilon_2^\infty \omega_1^2 \omega_3^2 + \epsilon_2^0(\omega_1^2 + \omega_3^2)]\cos^2\phi_2 + [\epsilon_3^\infty \omega_1^2 \omega_2^2 + \epsilon_3^0 \omega_3^2(\omega_1^2 + \omega_2^2)]\cos^2\phi_3}{\epsilon_1^\infty \cos^2\phi_1 + \epsilon_2^\infty \cos^2\phi_2 + \epsilon_3^\infty \cos^2\phi_3} \quad . \qquad (39)$$

SUMMARY AND CONCLUSIONS

The ω-versus-$\vec{k}$ relationship for a diatomic ionic orthorhombic crystal has been derived and is given by (15) and (17). As Huang has done for cubic crystals and Loudon for the uniaxial case, a retarded electromagnetic field, using the complete set of Maxwell's equations, has been used to interact with the vibrating lattice. The resultant vibration field was found to consist of a mixture of the electromagnetic radiation field and the lattice vibration field, as expected. In general, the frequency ω was found to be dependent upon the orientation (as well as the magnitude) of the wave vector $\vec{k}$ with respect to the crystal axes. The orientation is given by two angles.

Three cases illustrating special $\vec{k}$-vector direc-

tions have been considered; these three cases describe all possible situations for these orthorhombic crystals. It has been shown that all five ω-versus-$\vec{k}$ branches are explicitly given by the equations. Typical cases were computed and graphically illustrated. The ω-versus-$\vec{k}$ equations for uniaxial and cubic crystals have been obtained as special cases. Expressions are given for the change in the right-angle Raman scattering frequencies with $\vec{k}$-vector orientation change in orthorhombic crystals given.

[1]R. H. Lyddane, R. G. Sachs, and E. Teller, Phys. Rev. **59**, 673 (1941).

[2]K. Huang, Proc. Roy. Soc. (London) **A208**, 352 (1951); M. Born and K. Huang, *Dynamical Theory of Crystal Lattices* (Oxford, London, 1956).

[3]H. Poulet, Ann. Phys. (N. Y.) **12**, 908 (1955).

[4]L. Merten, Z. Naturforsch. **A15**, 47 (1960).

[5]R. Loudon, Advan. Phys. **13**, 423 (1964).

[6]A. S. Barker, Jr., Phys. Rev. **136**, A1290 (1964).

[7]See, for example, J. F. Nye, *Physical Properties of Crystals* (Oxford U. P., London, 1967).

Effect of Electric Field and Temperature on the Radiative Lifetime of the F Center[*][†]

L. F. Stiles, Jr.,[‡] M. P. Fontana, and D. B. Fitchen
Laboratory of Atomic and Solid State Physics, Cornell University, Ithaca, New York 14850
(Received 27 April 1970)

The lifetime of the excited F center at 4.2 °K and the changes in the radiative lifetime induced by an applied electric field and by increasing temperature have been measured in KCl, KF, and NaF with sufficient precision to test recent models for the relaxed excited states. The quantities measured were the luminescent decay time τ (using a pulse sampling technique), the relative luminescent yield η (using conventional techniques), and the emission-line-shape function. Changes in lifetime were measured for [100] applied dc fields of 0–140 kV/cm at 4.2 °K. These changes were of the form $\Delta\tau/\tau = -\beta F^2$, where F is the field in kV/cm, and β is $(5.8 \pm 0.5) \times 10^{-6}$ in KCl, $(4.0 \pm 0.3) \times 10^{-6}$ in KF, and $(3.0 \pm 0.3) \times 10^{-6}$ in NaF. Lifetime and yield were measured from 4.2 to 150 °K with approximately 1% precision. In KCl and KF, these data are used to demonstrate that the only two decay modes from the relaxed excited states are emission and thermal ionization, so that the radiative lifetime is τ/η. In NaF, another decay mode during relaxation appears to complicate the results, but the radiative lifetime can be extracted using additional data reported by Podini. In all three cases, the radiative lifetime decreases as the temperature increases. Both the electric field and the temperature effects on the radiative lifetime are quantitatively consistent with the mixed-state model recently proposed by Bogan in which the lowest emitting state is presumed to be $2s$-like, with a large admixture of $2p$ states. Values for the characteristic parameters, the mixing parameter α, and the level separation $\langle\delta E\rangle$ are determined from these data and agree with values determined in a different manner by Bogan.

I. INTRODUCTION

The F center in alkali halides consists of an electron trapped at a single halogen vacancy. Its presence in a crystal is characterized by several broad optical-absorption bands in or near the visible spectrum. Excitation in any of these absorption bands, at sufficiently low temperatures, leads to a single broad emission band. Although the F center has been studied for many decades, it is only very recently that an understanding of the states responsible for this emission is emerging.[1]

Swank and Brown[2] were the first to measure the decay time of the F-center luminescence. They found that the radiative lifetime of the excited center (F^*) was approximately two orders of magnitude longer than the value to be expected from the oscillator strength in absorption. Of the various explanations which they proposed for this discrepancy, the diffuse p-state model gained

wide acceptance as a result of the work of Fowler.[3] He was able to show that the Γ_4^- ($2p$-like) state of F^* would become more diffuse as the surrounding ions adjusted to the change in charge distribution following the optical excitation. This would reduce the matrix element for emission to the ground state. Using plausible values for an effective dielectric constant in a semicontinuum model, he was able to predict the right order of magnitude of the decay time.

However, the recent work of Bogan[4] and of Kühnert[5] could not be explained by the diffuse p-state model. Both these authors studied the Stark effect on the relaxed excited state of the F center by analyzing the electric-field-induced linear polarization of the luminescence. Their results implied that the luminescent state of F^* has a considerable amount of $2s$ character. Whether the relaxed excited state consisted of completely degenerate $2s$-$2p$ states, as assumed by Kühnert, or of strongly mixed but not degenerate states,